JOC Article

Substituent-Dependent Negative Hyperconjugation in 2-Aryl-1,3-*N*,*N*-heterocycles. Fine-Tuned Anomeric Effect?

Anasztázia Hetényi, Tamás A. Martinek, László Lázár, Zita Zalán, and Ferenc Fülöp*

Institute of Pharmaceutical Chemistry, University of Szeged, H-6701 Szeged, POB 121, Hungary

fulop@pharma.szote.u-szeged.hu

Received April 1, 2003

The epimerization reactions of conformationally inflexible 2-aryl-1,3-*N*,*N*-heterocycles were used as model systems to study the role of the nitrogen lone pair-C2 associated antibonding orbital hyperconjugative interactions in the experimentally observed substituent-dependent generalized anomeric effect. The measured reaction free enthalpies were found to correlate well with the sum of the hyperconjugative stabilization energies of all the vicinal donor−acceptor orbital overlaps around C2, obtained from ab initio NBO analysis, and both quantities correlated linearly with the Hammett−Brown substituent constant. The individual stereoelectronic interactions ($n_N-\sigma^*_{C2-N}$, $n_N-\sigma^*_{C2-Ar}$, $n_N-\sigma^*_{C2-H}$) were also observed to exhibit a substituent dependence, despite their distance from the 2-aryl substituent and their nonperiplanar arrangement. The higher the electron-withdrawing effect of the 2-aryl substituent, the larger was the stabilization for $n_N-\sigma^*_{C2-Ar}$, while the overlaps $n_N-\sigma^*_{C2-N}$ and $n_N-\sigma^*_{C2-H}$ changed in the opposite sense. The different polarization of the acceptor σ^* orbitals, caused by the 2-aryl substituent, accounted for the observed propagation of the substituent effect. These results promote a detailed explanation of the useful tautomeric behavior of the 2-aryl-1,3-*X*,*N*-heterocycles, and reveal the nature of the connection between the anomeric effect and the Hammett-type linear free energy relationship.

Introduction

The generalized anomeric effect (AE) is recognized in an Lp−X−A−Y moiety as a preference for an antiperiplanar arrangement of the lone pair (Lp) and the A−Y bond, where X is a heteroatom, A is an element with intermediate electronegativity (EN), and Y is a group with higher EN.[1,2] Despite the dispute continuing up to recent years concerning the exact origin of this well-established conformational phenomenon,[3,4] it is generally accepted that the stability difference observed between two specific geometries of the same molecular moiety stems from two-electron/two-orbital hyperconjugative interactions resulting in an excess stabilization energy.[5] There are four major factors that influence the excess of the electron delocalization energy: (i) the EN difference along the A−Y bond, (ii) the acceptor orbital energy level, (iii) the nature of the atom X, and (iv) the Lp−X−A−Y dihedral angles observed in the compared structures. Handling the stability difference as a function of the acceptor ability of the A−Y bond and that of the Lp−X−A−Y dihedral angle allows a further generalization of the concept. This approach has resulted in a number of studies involving the use of various functional groups as Y and elements with intermediate EN as A.[4,6,7] Despite the difficulties in the detection of the low energy differences in systems containing carbon as Y (e.g., −COR, −COOR, or −Ar),[8−10] it has been revealed that the stability difference between the C2 epimers in the epimerization equilibrium of 2-aryl-*trans*-1,3-*X*,*S*-decalins is affected by the electronic properties of the aromatic substituent.[11,12] In regard to the local geometry, observations of AE have been reported in conformations other than antiperiplanar.[13]

In this work, we intend to extend the application of the concept of AE. Using the epimerization equilibrium of 2-aryl-1,3-*N*,*N*-heterocycles as model system, we show that substituent-dependent stereoelectronic stabilization can occur even in a nonperiplanar arrangement and it can be characterized by the Hammett−Brown substituent constants by making use of linear free energy

* To whom correspondence should be addressed. Tel: +36-62-545564. Fax: +36-62-545705.

(1) Kirby, A. J. *The Anomeric Effect and Related Stereoelectronic Effects at Oxygen*; Springer-Verlag: Berlin, 1983.
(2) Juaristi, E.; Cuevas, G. *Tetrahedron* **1992**, *48*, 5019−5087.
(3) Salzner, U. *J. Org. Chem*. **1995**, *60*, 986−995.
(4) Carballeira, L.; Pérez-Juste, I. *J. Phys. Chem*. **2000**, *104*, 9362−9369.
(5) (a) Alabugin, I. V. J. *Org. Chem*. **2000**, *65*, 3910−3919. (b) Schleyer, P. v. R.; Kos, A. J. *Tetrahedron* **1983**, *39*, 1141−1150.
(6) Mikolajczyk, M.; Garaczyk, P.; Wieczorek, M. W.; Bujacz, G. *Angew. Chem., Int. Ed. Engl*. **1991**, *30*, 578−580.
(7) (a) Reed, A. E.; Schleyer, P. v. R. *J. Am. Chem. Soc*. **1987**, *109*, 7362−7373. (b) Alabugin, I. V.; Zeidan, T. A. *J. Am. Chem. Soc*. **2002**, *124*, 3475−3185.
(8) Anderson, C. B.; Sepp, D. T. *J. Org. Chem*. **1968**, *33*, 3272−3276.
(9) Juaristi, E.; Tapia, J.; Méndez, R. *Tetrahedron* **1986**, *42*, 1253−1264.
(10) Juaristi, E.; González, E. A.; Pinto, B. M.; Johnston, B. D.; Nagelkerke, R. *J. Am. Chem. Soc*. **1989**, *111*, 6745−6749.
(11) Tschierske, C.; Köhler, H.; Zaschke, H.; Kleinpeter, E. *Tetrahedron* **1989**, *45*, 6987−6998.
(12) Köhler, H.; Tschierske, C.; Zaschke, H.; Kleinpeter, E. *Tetrahedron* **1990**, *46*, 4241−4246.
(13) King, J. F.; Rathore, R.; Guo, Z.; Li, M.; Payne, N. C. *J. Am. Chem. Soc*. **2000**, *122*, 10308−10324.

10.1021/jo034417+ CCC: $25.00
Published on Web 06/06/2003

SCHEME 1

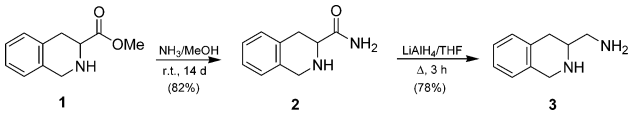

relationship (LFER) analysis. The results of the ab initio calculations performed, including the natural bond orbital (NBO)[14−17] method, shed considerable light on the mechanism of propagation of the influence of the 2-aryl substituent on the ring stability of the 1,3-*N*,*N*-heterocycles due to substituent-dependent hyperconjugative interactions.

Results and Discussion

The Model Compounds. The 1,3-*X*,*N*-heterocycles are apt to participate in equilibrium processes involving opening of the heterocyclic ring at C2. These processes include ring−ring epimerization and ring−chain tautomerism.[18] The early works of Kleinpeter et al.,[11,12] our own previous studies on 2-aryl-1,3-*X*,*N*-heterocycles,[19] and the recent work of Neuvonen et al.[20] turned our attention to the fact that not only the ring-chain equilibrium ratios but also the ring−ring epimerization equilibrium can be influenced by the 2-aryl substituent. The substituent dependence of the ring stability is affected by the relative configuration of C2, and thus, this stability difference presumably caused by an AE can be separated experimentally. We assumed that the observation of the substituent-dependent AE is related to the conformational rigidity of the 1,3-*N*,*N*-heterocycles caused by the condensed ring system and the tertiary nitrogen substituted by sterically demanding groups. Therefore, inflexible model compounds **11**−**14** containing a tertiary nitrogen in ring annelation were synthesized from the corresponding 1,2,3,4-tetrahydroisoquinoline-1- or 3-methylamines.[21] 3-Aminomethyl-1,2,3,4-tetrahydroisoquinoline **3**, necessary for the linear imidazoisoquinoline model compounds, was synthesized by reduction of the corresponding carboxamide **2** (Scheme 1) obtained from the easily available amino ester **1**.[22]

1-Aminomethyl-6,7-dimethoxy-1,2,3,4-tetrahydroisoquinoline **8**, the starting material for the synthesis of angularly condensed imidazoisoquinoline model compounds, was prepared in four steps, starting from N-protected glycine **4** and homoveratrylamine (Scheme 2).

SCHEME 2

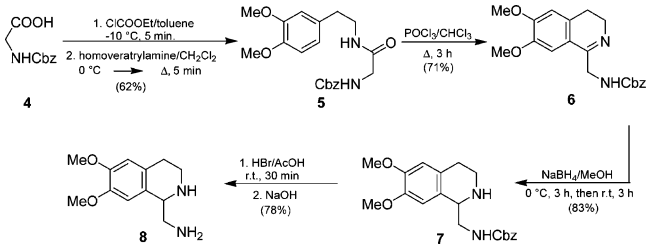

SCHEME 3

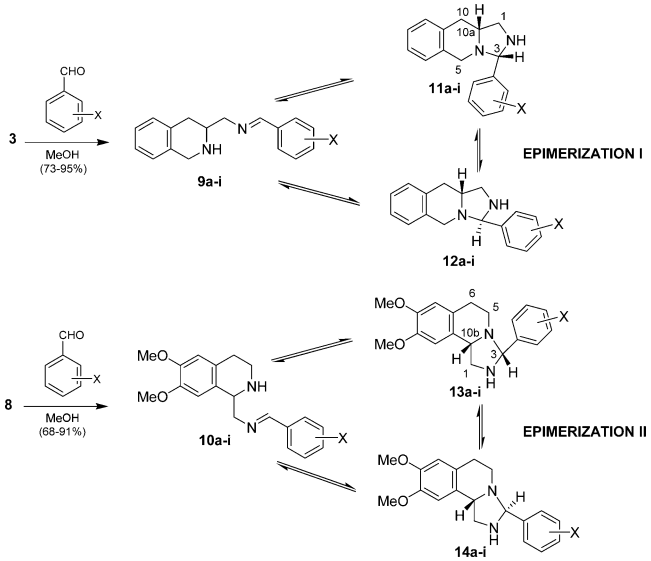

X = **a**, *p*-NO_2; **b**, *p*-CF_3; **c**, *p*-Br; **d**, *p*-Cl; **e**, H; **f**, *p*-F; **g**, *p*-Me; **h**, *p*-OMe; **i**, *p*-NMe_2

In contrast with the great number of imidazo[5,1-*a*]- and imidazo[1,5-*b*]isoquinolines bearing oxo/thioxo substituents or sp^2 carbons at positions 1 and/or 3,[24,25] only one recent publication is known that relates to the synthesis of the saturated analogues with sp^3 carbons in those positions.[26]

The condensations of diamines **3** and **8** with equivalent amounts of nine aromatic aldehydes in $CDCl_3$ at 300 K resulted in three-component tautomeric mixtures **9**, **11**, **12** and **10**, **13**, **14** (two C-3 epimeric imidazoisoquinolines and the corresponding Schiff base) (Scheme 3), containing angularly and linearly condensed imidazoisoquinolines in epimerization equilibria.

(14) Salzner, U.; Schleyer, P. R. *J. Org. Chem*. **1994**, *59*, 2138−2155.
(15) Cortés, F.; Tenorio, J.; Collera, O.; Cuevas, G. *J. Org. Chem*. **2001**, *66*, 2918−2924.
(16) Reed, E. A.; Weinstock, R. B.; Weinhold, F. *J. Chem. Phys*. **1985**, *83*, 735−746.
(17) Reed, E. A.; Curtiss, L. A.; Weinhold, F. *Chem. Rev*. **1988**, *88*, 899−926.
(18) (a) Valters, R. E.; Flitsch, W. *Ring-Chain Tautomerism*; Plenum Press: New York, 1985. (b) Valters, R. E.; Fülöp, F.; Korbonits, D. *Adv. Heterocycl. Chem*. **1996**, *66*, 1.
(19) Lázár, L.; Göblyös, A.; Martinek, T. A.; Fülöp, F. *J. Org. Chem*. **2002**, *67*, 4734−4741.
(20) Neuvonen, K.; Fülöp, F.; Neuvonen, H.; Koch, A.; Kleinpeter, E.; Pihlaja K. *J. Org. Chem*. **2001**, *66*, 4132−4140.
(21) Schuster, H.; Kathawala, F. G. Isoquinolines Bearing Basic Side Chains. In *The Chemistry of Heterocyclic Compounds, Vol. 38, Isoquinolines*; Coppola, G. M., Schuster, H. F., Eds.; Wiley: New York, 1995; Part 3, p 1.
(22) (a) Hayashi, K.; Ozaki, Y.; Nunami, K.; Yoneda N. *Chem. Pharm. Bull*. **1983**, *31*, 312−314. (b) Grunewald, G. L.; Sall, D. J.; Monn, J. A. *J. Med. Chem*. **1988**, *31*, 824−830.
(23) Compounds **1**−**3** and **7**−**14** are racemates. In the schemes, only the enantiomers of **10**−**14** having the annelation hydrogen in the β position are shown.
(24) (a) Liao, Z.; Kohn, H. *J. Org. Chem*. **1984**, *49*, 4745−4752. (b) Kano, S.; Yuasa, Y.; Shibuya, S. *Synth. Commun*. **1985**, *15*, 883−889. (c) Jones, R. C. F.; Smallridge, M. J.; Chapleo, C. B. *J. Chem. Soc., Perkin Trans. 1* **1990**, 385−391. (d) Fülöp, F.; Semega, É.; Bernáth, G.; Sohár, P. *Pharmazie* **1992**, *47*, 168−171. (e) Collado, M. I.; Sotomayor, N.; Villa, M.; Lete, E. *Tetrahedron Lett*. **1996**, *37*, 6193−6196. (f) Osante, I.; Collado, M. I.; Lete, E.; Sotomayor, N. *Eur. J. Org. Chem*. **2001**, 1267−1277. (g) Funabashi, K.; Ratni, H.; Kanai, M.; Shibasaki, M. *J. Am. Chem. Soc*. **2001**, *123*, 10784−10785.
(25) (a) Weir, E. C.; Niopas, I.; Smail, G. A. *Chem. Chron*. **1989**, *18*, 3−17. (b) Albanoudi, A.; Gabrieli, C.; Niopas, I. *Sci. Pharm*. **1990**, *58*, 259−262. (c) Niopas, I.; Smail, G. A. *J. Chem. Soc., Perkin Trans. 1* **1991**, 113−117. (d) Wu, S.; Janusz, J. M.; Sheffer, J. B. *Tetrahedron Lett*. **2000**, *41*, 1159−1163. (e) Charton, J.; Delarue, S.; Vendeville, S.; Debreu-Fontaine, M.; Girault-Mizzi, S.; Sergheraert, C. *Tetrahedron Lett*. **2001**, *42*, 7559−7561.
(26) Katritzky, A. R.; Suzuki, K.; He, H.-Y. *J. Org. Chem*. **2002**, *67*, 8224−8229.

TABLE 1. Proportions (%) of Tautomeric Forms in Tautomeric Equilibria for Compounds 9−14 ($CDCl_3$, 300 K)

compd	X	σ^+	**9**	**11**	**12**	**10**	**13**	**14**
a	*p*-NO_2	0.79	3.4	88.7	7.9	4.1	25.8	70.1
b	*p*-CF_3	0.612	4.8	88.2	7.0	4.7	32.0	63.3
c	*p*-Br	0.15	7.6	86.1	6.3	14.7	28.9	56.4
d	*p*-Cl	0.114	6.9	88.0	5.1	8.1	38.1	53.8
e	H	0	9.0	86.3	4.7	12.8	28.1	59.1
f	*p*-F	−0.073	9.6	85.4	5.0	9.9	38.6	51.5
g	*p*-Me	−0.311	11.6	85.0	3.4	14.3	28.9	56.8
h	*p*-OMe	−0.778	14.3	82.5	3.2	24.3	29.5	46.2
i	*p*-NMe_2	−1.7	34.6	63.7	1.7	57.0	14.6	28.4

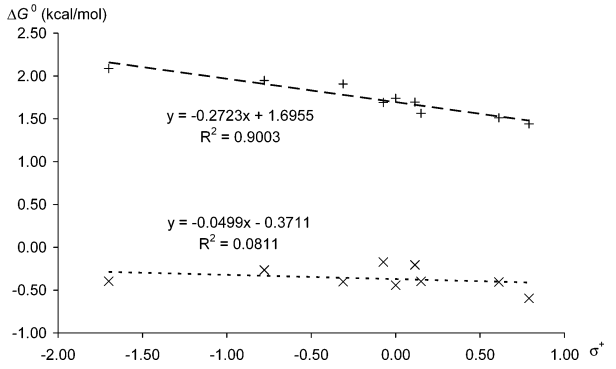

FIGURE 1. Plots of ΔG^0 vs Hammett-Brown σ^+ values for epimerizations I (+) and II (×).

After the attainment of equilibrium, the specta of compounds **9a**−**i** or **10a**−**i** contained well-separated singlets resonating from the azomethine group at 8.31−8.46 ppm or 8.23−8.44 ppm and the two N−C*H*Ar−NH hydrogens in the region 4.11−4.63 or 4.22−4.92 ppm. With the aim of an unambiguous signal assignment, standard 2D homo- and heteronuclear spectra were recorded. Selected ^{1}H chemical shifts for some characteristic nuclei are presented in Table S1 (Supporting Information). The proportions K_X of the chain (**9**, **10**) and diastereomeric ring forms (**11**, **13** and **12**, **14**) of the tautomeric equilibria **9a**−**i** and **10a**−**i** were determined by integration of the well-separated N=C*H*Ar (chain) and N−C*H*Ar−NH (ring) proton singlets in the ^{1}H NMR spectra (Table 1).

LFER analysis of the reaction free energies (Scheme 3, calculated at 300 K) demonstrates an acceptable linear correlation with the Hammett−Brown substituent constants (σ^+) for epimerization I, while the linear fit falls off for epimerization II (Figure 1).

The conformationally restrained condensed ring systems **11** and **12** display significant substituent effects on the epimerization equilibrium, but the angularly condensed imidazoisoquinolines **13** and **14** do not exhibit net substituent effects on the relative stabilities. Our conclusion at this point is that the selected models are suitable for detailed analysis of the stereoelectronic interactions probably responsible for the substituent-dependent AE.

Conformational Analysis. Since the stereoelectronic interactions are highly dependent on the geometry of the studied molecules, thorough conformational analysis was performed. Our goal was to determine the predominant geometry for all the models and to identify the possible minor conformers influencing the correlation between the calculated and the measured data. The conformational search protocol comprised a stochastic search using the Merck Molecular Force Field (MMFF94)[27] and a subsequent minimization of the resulting low-energy conformations at the ab initio level, using the HF/3-21G* basis set for all the compounds **11**(**a**−**i**)−**14**(**a**−**i**). The resulting structures proved to be rigid, since no minor conformation was found within the 6 kcal/mol energy window. The final conformations for **11e**−**14e** are shown in Figure 2.

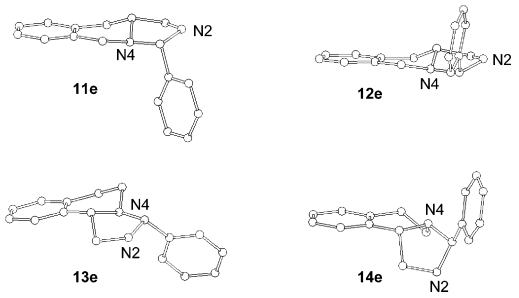

FIGURE 2. Final predominant minimum energy molecular structures for **11e**−**14e**, obtained by using ab initio HF/3-21G* calculations.

The conformations obtained are supported by the NOE patterns determined via the NOESY spectra. It is clear from the structures that the ideal, antiperiplanar arrangement cannot be found for the nitrogen lone pairs and the possible endocyclic and exocyclic substituents on C3.

NBO Analysis. The exact analysis of the delocalization energy contributions to the substituent-dependent AE is a complex problem which can be tackled through a second-order perturbative analysis of the Fock matrix in the NBO basis. Although this procedure is known to overestimate stabilizing interactions, they closely parallel the energies afforded by the more accurate Fock matrix deletion method.[7b,28] The second-order energy stabilization due to the electron donation from orbital *i* to orbital *j* is given by eq 1, where q_i is the donor orbital occupancy, ϵ_i and ϵ_j are diagonal elements, and F_{ij} is the off-diagonal NBO Fock matrix element. The NBO calculations were performed at the HF/6-31G* level using geometries optimized at the HF/3-21G* level.

$$E_{ij} = q_i \frac{F_{ij}^2}{\epsilon_j - \epsilon_i} \qquad (1)$$

In the present model compounds, each nitrogen lone pair can overlap with three different vicinal antibonding orbitals associated with C3: namely σ^*_{C3-N}, σ^*_{C3-Ar}, and σ^*_{C3-H}. (From here, the exact numbering of the model ring system is followed.) Since we were interested in the 3-aryl substituent-dependent stereoelectronic interactions, six orbital overlaps around C3 were taken into consideration in our analysis. The results of the NBO calculations revealed an insignificant amount of stabilization energy for $n_{N4}-\sigma^*_{C3-N}$ and $n_{N2}-\sigma^*_{C3-H}$ in **11**, for $n_{N4}-\sigma^*_{C3-N}$, $n_{N4}-\sigma^*_{C3-H}$, $n_{N2}-\sigma^*_{C3-N}$, and $n_{N2}-\sigma^*_{C3-H}$ in **12**, for $n_{N4}-\sigma^*_{C3-N}$ and $n_{N2}-\sigma^*_{C3-H}$ in **13**, and for $n_{N4}-\sigma^*_{C3-H}$ and $n_{N2}-\sigma^*_{C3-H}$ in **14**, which was accompanied by

(27) Halgren, T. A. *J. Comput. Chem.* **1996**, *17*, 490−519.
(28) Arnaud, R. *J. Comput. Chem.* **1994**, *15*, 1341−1356.

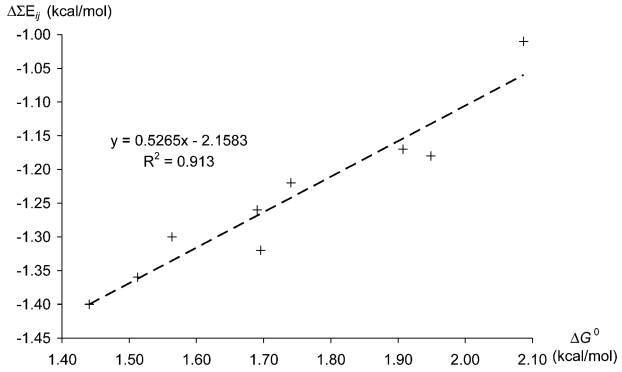

FIGURE 3. Plots of theoretical stereoelectronic stabilization energy $\Delta\sum E_{ij}$ vs ΔG^0 values for epimerization I.

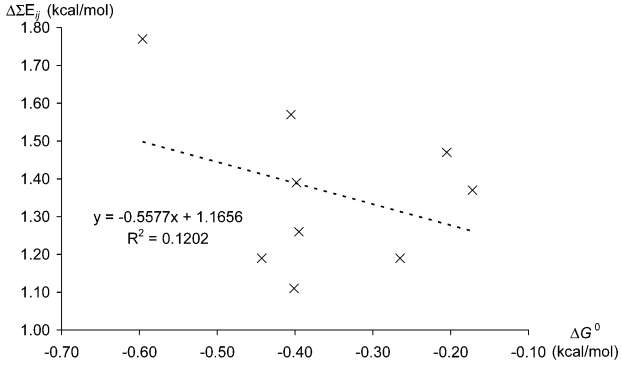

FIGURE 4. Plots of theoretical stereoelectronic stabilization energy $\Delta\sum E_{ij}$ vs ΔG^0 values for epimerization II.

a negligible variation. The signed sum of the E_{ij} values gives the theoretical hyperconjugative stabilization energy $\Delta\sum E_{ij}$ in eq 2, where r and l designate the right-hand side and the left-hand side, respectively, of the epimerization equilibria.

$$\Delta\sum E_{ij} = \sum E^r_{ij} - \sum E^l_{ij} \qquad (2)$$

To correlate the experimental stability differences with the theoretical results, linear regression analysis was carried out with $\Delta\sum E_{ij}$ against ΔG^0 (Figures 3 and 4).

For epimerization I, we obtained a good linear relationship, while in the case of epimerization II there was no significant correlation. The variances of ΔG^0 and $\Delta\sum E_{ij}$ were of the same magnitude and the linear correlations were acceptable for epimerization I. These findings suggest that the observed 3-aryl substituent-dependent stability difference is stereoelectronic in origin. The lack of any linear relationship for epimerization II indicates that the variations in ΔG^0 cannot be explained by an electron delocalization energy excess. The correlation between $\Delta\sum E_{ij}$ and σ^+ exhibits a similar pattern (Figure 5). The regression analysis for epimerization I gave a linear fit, while $\Delta\sum E_{ij}$ for epimerization II proved independent of σ^+, which is in good agreement with the experimental observations.

It is clear that the experimentally detected substituent-dependent stability difference for epimerization I is connected with the AE comprising all the possible n$-\sigma^*$ interactions around C3. For epimerization II, the electronic properties of the 3-aryl substituent do not seem to exert a detectable effect either on the experimental

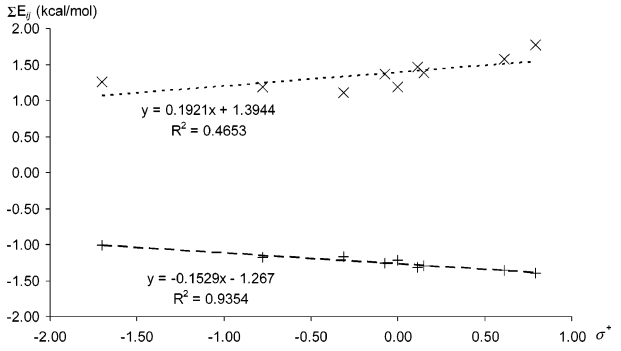

FIGURE 5. Plots of theoretical stereoelectronic stabilization energy $\Delta\sum E_{ij}$ vs Hammett−Brown σ^+ values for epimerizations I (+) and II (×).

reaction free energy or on the calculated stereoelectronic stabilization energy. These results raise two questions: (i) Are the electron delocalization energies of the individual orbital overlaps also substituent-dependent? (ii) What specific NBO donor−acceptor interactions are responsible for the substituent-dependent stabilization?

The Hammett−Brown substituent dependence of the E_{ij} values was tested by univariate linear regression for both epimerization equilibria. The calculation was carried out for each NBO donor−acceptor interaction, and the summary of the analysis is displayed in Table 2; all the linear fits exceeding a significance limit of 99% are given.

The results demonstrate that, regardless of the nature of the antibonding orbitals associated with C3, the 3-aryl substituent can have a significant influence on the two orbital electron delocalization energies, even in compounds **13** and **14**. It is also seen that the σ^+ values are in an acceptably linear correlation with the E_{ij} values, despite the fact that the interacting orbitals are not in a periplanar conformation. The evaluation of the slope of the linear models (ρ) demonstrates that the 3-aryl substituents have a strong positive influence on the $n_N-\sigma^*_{C3-Ar}$ interaction energies, i.e., the higher the value of σ^+, the higher the absolute value of the stabilization energy. It is interesting that the interactions $n_N-\sigma^*_{C3-N}$ and the $n_N-\sigma^*_{C3-H}$ change in an opposite sense: electron-withdrawing substituents decrease the stabilizating delocalization energy. The $n_N-\sigma^*_{C3-H}$ overlaps are subjected to a weak modulation by σ^+ as compared with those obtained for $n_N-\sigma^*_{C3-Ar}$.

Our observations reveal that all the possible vicinal n$-\sigma^*$ interactions around C3 that have a conformational arrangement other than orthogonal may contribute to the substituent-dependent AE (Figure 6).

Translating the results of the NBO analysis to the language of the valence bond theory gives an intuitive picture of three types of double bond−no bond resonance structures responsible for the phenomenological behavior of the studied models (Scheme 4).

The growing electron demand of the 3-aryl substituent increases the stabilizing contribution of the resonance structure **B**, while the weights of the negative hyperconjugations **C** and **D** taper off. Depending on the exact geometry of the species in the epimerization equilibrium, the influence of the substituent on the donor−acceptor interactions can result overall in an experimentally observable substituent dependence of the equilibrium

TABLE 2. Summary of the Linear Regression Analysis for the Hammett−Brown Substituent Dependence of the Hyperconjugative Stabilization Energy (E_{ij}) Values and Dihedral Angles between the Interacting Orbitals (θ)

E_{ij}		**11**	**12**	**13**	**14**
$n_{N2}-\sigma^*_{C3-Ar}$	r	0.91	0.92	0.92	0.97
	ρ^b (kcal/mol)	−0.54 ± 0.09	−0.28 ± 0.04	−0.51 ± 0.08	−0.49 ± 0.04
	C^b (kcal/mol)	−5.52 ± 0.07	−5.51 ± 0.03	−4.88 ± 0.06	−4.78 ± 0.03
	θ (deg)	131.49	−25.64	128.16	−26.20
$n_{N2}-\sigma^*_{C3-N4}$	r	0.94	*a*	0.94	0.97
	ρ^b (kcal/mol)	0.25 ± 0.04	*a*	0.28 ± 0.04	0.32 ± 0.03
	C^b (kcal/mol)	−0.82 ± 0.03	*a*	−1.13 ± 0.03	−7.88 ± 0.02
	θ (deg)	−72.23	−83.15	68.12	146.02
$n_{N2}-\sigma^*_{C3-H}$	r	*a*	*a*	*a*	*a*
	ρ (kcal/mol)^b	*a*	*a*	*a*	*a*
	C (kcal/mol)^b	*a*	*a*	*a*	*a*
	θ (deg)	−10.42	147.29	6.82	84.74
$n_{N4}-\sigma^*_{C3-Ar}$	r	0.93	0.85	0.93	0.97
	ρ (kcal/mol)^b	−0.42 ± 0.06	−0.45 ± 0.10	−0.43 ± 0.06	−0.20 ± 0.02
	C (kcal/mol)^b	−5.13 ± 0.05	−7.97 ± 0.08	−4.62 ± 0.04	−2.75 ± 0.01
	θ (deg)	−27.19	140.29	33.94	38.53
$n_{N4}-\sigma^*_{C3-N2}$	r	*a*	*a*	*a*	0.92
	ρ (kcal/mol)^b	*a*	*a*	*a*	−0.05 ± 0.01
	C (kcal/mol)^b	*a*	*a*	*a*	−9.45 ± 0.01
	θ (deg)	−86.11	−80.16	93.46	158.90
$n_{N4}-\sigma^*_{C3-H}$	r	0.89	*a*	0.85	*a*
	ρ (kcal/mol)^b	0.13 ± 0.02	*a*	0.07 ± 0.02	*a*
	C (kcal/mol)^b	−8.32 ± 0.02	*a*	−9.58 ± 0.01	*a*
	θ (deg)	149.6	−19.05	156.99	61.29

[a] Significance level is below 99%. [b] Regression was calculated for the linear model: $E_{ij} = \rho\sigma^+ + C$.

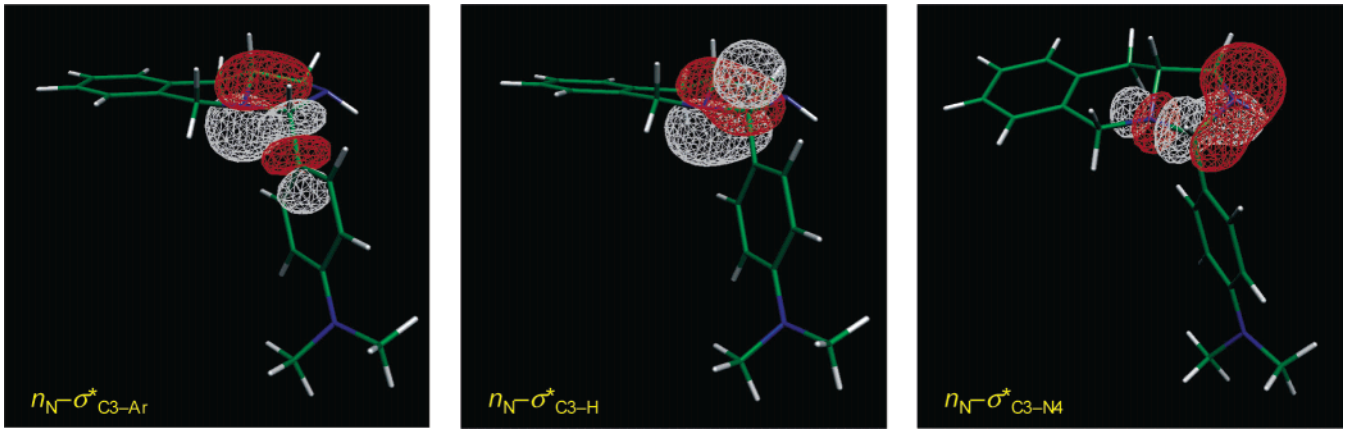

FIGURE 6. Graphical representations of the selected NBO interactions contributing to the substituent-dependent stereoelectronic stabilization. The orbital overlaps are displayed for **11i**.

SCHEME 4

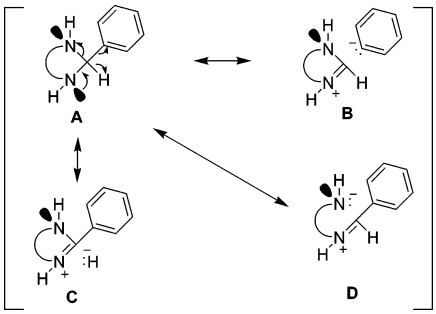

ratios (epimerization I), which may be interpreted as a fine-tuned AE. It is also possible that the individual hyperconjugative contributions cancel out, leading to an equilibrium ratio that is independent of σ^+ (epimerization II).[29]

Equation 1 contains two important parameters determining the E_{ij} values: the reciprocal donor−acceptor orbital energy difference ($\Delta\epsilon = \epsilon_j - \epsilon_i$) and the square of the NBO Fock matrix off-diagonal element (F_{ij}). $\Delta\epsilon^{-1}$ changes in parallel with σ^+ for all types of acceptor orbitals, and the relative increase in $\Delta\epsilon^{-1}$ on going from *p*-NMe_2 to *p*-NO_2 is only a few percent (Figure 7).

This is in accordance with the picture of decreasing acceptor orbital energy due to the increasing electron-withdrawing effect of the 3-aryl substituent. Inspection

(29) The substituent effects of the 8,9-methoxy substituents in compounds **10**, **13**, and **14** a priori cannot be ruled out. Since the aromatic group is two bonds away from the C3−N4 bond, it might perturb the polarization of this bond, and hence it may change the stereoelectronic stabilization energy. Since the model compounds in question are symmetric in that the aromatic substituent on C3 is also at a distance of two bonds from the C10b−N4 bond, the substituent effect in such cases can be estimated by using the results of our calculations. For investigation of the influence on the polarization coefficient of the C10b sp^3 atomic orbitals Figure S1 was prepared. It is seen that the polarization of $\sigma^*_{C10b-Ar}$ and $\sigma^*_{C10b-N4}$ can be considered to be independent from the σ^+ values. This suggests that the methoxy groups are unlikely to influence the substituent-dependent stereoelectronic stabilization revealed by our analysis.

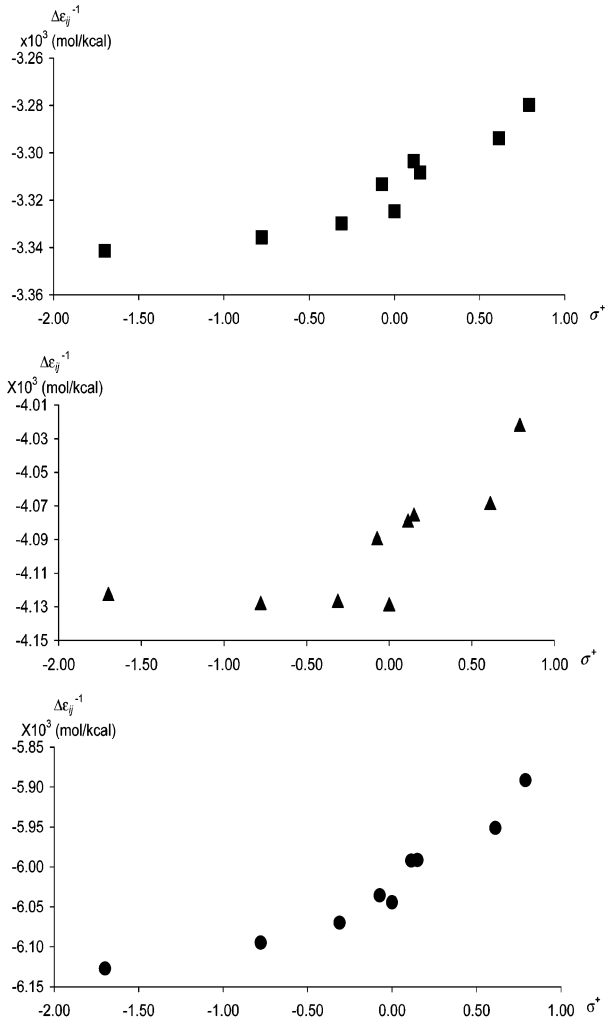

FIGURE 7. Plots of selected reciprocal donor−acceptor orbital energy difference ($\Delta\epsilon^{-1}$) in **11** obtained from NBO calculation. The symbols ■, ▲, and ● designate the orbital overlaps n_{N2}−σ^*_{C3-N4}, n_{N2}−σ^*_{C3-Ar}, and n_{N2}−σ^*_{C3-H}, respectively.

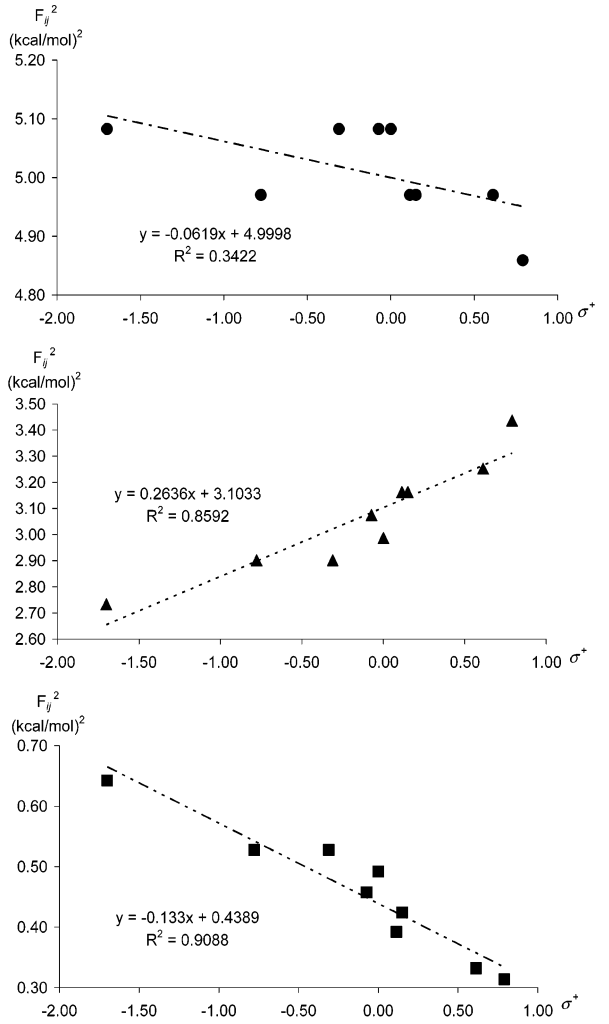

FIGURE 8. Plots of selected squared Fock matrix off-diagonal elements (F_{ij}^2) in **11** obtained from NBO calculations. The symbols ■, ▲, and ● designate the orbital overlaps n_{N2}−σ^*_{C3-N4}, n_{N2}−σ^*_{C3-Ar}, and n_{N2}−σ^*_{C3-H}, respectively.

of the substituent dependence of F_{ij}^2 (Figure 8) allows the conclusion that the changes in E_{ij} are mainly explained by the variations in F_{ij}, since the changes are higher as compared with those in $\Delta\epsilon^{-1}$, and the opposite trend of the correlation with σ^+ can also be detected. We note that the Fock matrix off-diagonal element for the n_N−σ^*_{C3-H} overlap does not exhibit a good linear fit against σ^+.

F_{ij} is strongly correlated with the orbital overlap matrix element S_{ij}, which finally boils down to a dihedral angle and acceptor orbital polarization dependence.[7b] The substituent-dependent conformational changes for these model compounds are around 1°, i.e., negligible. However, the polarization coefficients of the C3 sp^3 atomic orbitals increase in σ^*_{C3-Ar} and decrease in the acceptor bonds σ^*_{C3-N} and σ^*_{C3-H} when the electron demand of the 3-aryl substituent is augmented (Figure 9).

To summarize, the 3-aryl substituent effect contracts or expands the antibonding orbital in the direction of the donor lone pairs (Figure 10), which accounts exactly for the opposite trends of the variations in F_{ij}, and thus for the observed substituent dependence of the individual orbital overlap stabilization energies.

Conclusion

This extended view of the stereoelectronic interactions affords a detailed description of the substituent-dependent stability changes exhibited by the 2-aryl-1,3-*X*,*N*-heterocycles. The electron-withdrawing properties of the 2-aryl substituent alter the polarization along all the single bonds associated with C2; it therefore changes the extent of the orbital overlaps between the nitrogen lone pairs and the antibonding orbitals. The donor−acceptor hyperconjugative stabilization energies display an acceptable linear correlation with the Hammett−Brown substituent constant, and the theoretical stereoelectronic stabilization energies calculated as the sum of the individual orbital overlap electron delocalization energies explain the experimentally observed substituent-dependent AE.

Application of the results presented in this work may help resolve the question of the substituent dependence of the epimerization equilibrium constants in the field of ring-chain tautomerism. In accord with the currently increasing interest in dynamic covalent bonds allowing the construction of supramolecular structures and com-

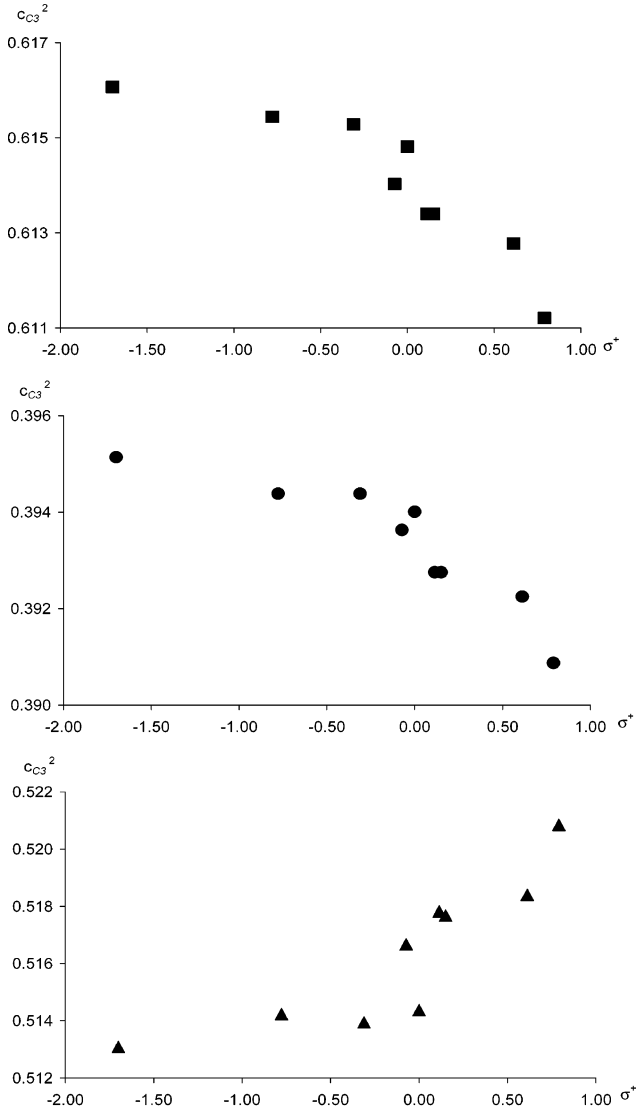

FIGURE 9. Substituent dependence of the polarization coefficients in the C3-associated antibonding orbitals in **11**. The symbols ■, ▲, and ● designate the orbital overlaps σ^*_{C3-N4}, σ^*_{C3-Ar}, and σ^*_{C3-H}, respectively.

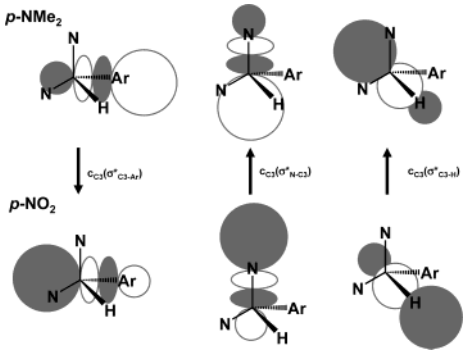

FIGURE 10. Graphical interpretation of the substituent dependence of the polarization coefficients on C3. On going from *p*-NMe_2 to *p*-NO_2, the C3−Ar antibonding orbital expands, while the C3−N and C3−H antibonding orbitals contract at C3.

binatorial libraries under equilibrium conditions,[30] the condensed 2-aryl-1,3-*X*,*N*-heterocycle derivatives were recently recognized as useful building blocks for the synthesis of novel supramolecular host compounds and dynamic combinatorial libraries.[31] It therefore appears important to provide explanations as to the exact electronic mechanisms of the effects exerted by the substituents and the stereochemistry on the equilibrium processes of these compounds.

Experimental Section

Compound **1**[22a] was prepared according to known procedures.

1,2,3,4-Tetrahydroisoquinoline-3-carboxamide (2). To a solution of amino ester **1** (7.65 g, 40 mmol) in MeOH (25 mL) was added 25% methanolic ammonia solution (100 mL). The mixture was allowed to stand in a well-closed container at ambient temperature for 14 days, and the solvent was then evaporated off. The crystalline product was filtered off, washed with Et_2O, dried, and recrystallized from EtOAc−EtOH: yield 5.78 g (82%); mp 164−166 °C (lit.[22b] mp 162−163 °C). The ^1H NMR data on the product correspond to the literature[22b] data.

3-Aminomethyl-1,2,3,4-tetrahydroisoquinoline Dihydrochloride (3·2HCl). To a stirred and cooled suspension of $LiAlH_4$ (2.85 g, 75 mmol) in dry THF (100 mL) was added carboxamide **2** (4.41 g, 25 mmol) in small portions. The mixture was stirred and refluxed for 3 h and then cooled, and the excess of $LiAlH_4$ was decomposed by the addition of a mixture of water (5.7 mL) and THF (40 mL). The inorganic salts were filtered off and washed with EtOAc (3 × 100 mL). The combined organic filtrate and washings were dried (Na_2SO_4) and evaporated under reduced pressure to give crude diamine **3** as an oil, which was converted to the crystalline dihydrochloride salt by treatment of its solution in MeOH with an excess of 22% ethanolic HCl and Et_2O. The crystalline dihydrochloride was filtered off, dried, and recrystallized from MeOH−H_2O−Et_2O: yield 4.61 g (78%); mp 244−247 °C; ^1H NMR (D_2O) δ 3.14 (dd, 1H, J = 10.8, 17.1 Hz), 3.37 (dd, 1H, J = 4.8, 16.4 Hz), 3.47 (dd, 1H, J = 6.8, 13.9 Hz), 3.59 (dd, 1H, J = 6.3, 13.9 Hz), 4.1 (ddd, 1H, J = 6.0, 11.3 Hz), 4.54 (s, 2H), 7.25−7.42 (m, 4H). Anal. Calcd for $C_{10}H_{16}Cl_2N_2$: C, 51.08; H, 6.86; N, 11.91. Found: C, 50.88; H, 6.61; N, 11.73.

α-Benzyloxycarbonylamino-*N*-[2-(3,4-dimethoxyphenyl)ethyl]acetamide (5). To a stirred and cooled (ice−salt bath) solution of *N*-(benzyloxycarbonyl)glycine (**4**, 10.46 g, 50 mmol) and Et_3N (5.06 g, 50 mol) in anhydrous toluene (100 mL) was added ethyl chloroformate (5.43 g, 50 mmol) dropwise at a rate low enough to keep the internal temperature below −10 °C. After 5 min, a solution of 2-(3,4-dimethoxyphenyl)-ethylamine (9.06 g, 50 mmol) in dry CH_2Cl_2 (50 mL) was added dropwise to the mixture, the internal temperature being kept below 0 °C. When the addition was complete, the reaction mixture was slowly heated to reflux and refluxed for 5 min. The mixture was allowed to cool to room temperature and washed with saturated aqueous $NaHCO_3$ solution (2 × 50 mL) and water (2 × 50 mL) after the addition of $CHCl_3$ (200 mL). The combined organic phases were dried (Na_2SO_4) and evaporated in vacuo to give a crystalline product, which was filtered off, washed with Et_2O, dried, and recrystallized from EtOAc: yield 11.55 g (62%); mp 122−124 °C; ^1H NMR ($CDCl_3$) δ 2.75 (t, 2H, J = 7.1 Hz), 3.51 (dd, 2H, J = 7.1, 13.1 Hz), 3.81 (d, 2H, J = 5.5 Hz), 3.85 (s, 3H), 3.87 (s, 3H), 5.11 (s, 2H), 5.30 (br s, 1H), 5.93 (br s, 1H), 6.67−6.73 (m, 2H), 6.79 (d, 1H, J = 8.6 Hz), 7.30−7.39 (m, 5H). Anal. Calcd for $C_{20}H_{24}N_2O_5$: C, 64.50; H, 6.50; N, 7.52. Found: C, 64.23; H, 6.37; N, 7.48.

1-Benzyloxycarbonylaminomethyl-6,7-dimethoxy-3,4-dihydroisoquinoline (6). To a stirred solution of compound

(30) Rowan, S. J.; Cantrill, S. J.; Cousins, G. R. L.; Sanders, J. K. M.; Stoddart, J. F. *Angew. Chem., Int. Ed.* **2002**, *41*, 898−952.

(31) (a) Star, A.; Goldberg, I.; Fuchs, B. *Angew. Chem., Int. Ed.* **2000**, *39*, 2685−2689. (b) Star, A.; Fuchs, B. *J. Org. Chem.* **1999**, *64*, 1166−1172.

5 (11.17 g, 30 mmol) in dry $CHCl_3$ (150 mL) was added $POCl_3$ (13.80 g, 90 mmol). The mixture was refluxed for 3 h and then evaporated. The oily residue was dissolved in hot water (200 mL), and the cooled solution was washed with EtOAc (2 × 50 mL). The aqueous phase was made alkaline with 20% NaOH under cooling and extracted with $CHCl_3$ (3 × 100 mL). The combined organic extracts were dried (Na_2SO_4) and evaporated in vacuo to give a crystalline product, which was filtered off, washed with Et_2O, dried, and recrystallized from MeOH: yield 7.55 g (71%); mp 123−126 °C; ^{1}H NMR ($CDCl_3$) δ 2.66 (t, 2H, J = 7.1 Hz), 3.69 (t, 2H, J = 7.6 Hz), 3.89 (s, 3H), 3.92 (s, 3H), 4.39−4.44 (m, 2H), 5.15 (s, 2H), 6.31 (br s, 1H), 6.70 (s, 1H), 6.94 (s, 1H), 7.28−7.42 (m, 5H). Anal. Calcd for $C_{20}H_{22}N_2O_4$: C, 67.78; H, 6.26; N, 7.90. Found: C, 67.99; H, 6.35; N, 7.68.

1-Benzyloxycarbonylaminomethyl-6,7-dimethoxy-1,2,3,4-tetrahydroisoquinoline (7). To a stirred and ice-cooled suspension of dihydroisoquinoline **6** (7.08 g, 20 mmol) in MeOH (100 mL) was added $NaBH_4$ (2.27 g, 60 mmol) in small portions. The mixture was stirred for 3 h with cooling and for 3 h without and then evaporated, and the residue was dissolved in 5% HCl (150 mL). The solution was made alkaline with 20% NaOH under ice cooling and extracted with $CHCl_3$ (4 × 100 mL). The combined organic extracts were dried (Na_2SO_4) and evaporated in vacuo to give crude **7** as an oil, which crystallized on treatment with *n*-hexane−Et_2O. The crystals were filtered off, washed with Et_2O, and used in the next step without further purification, yield 5.92 g (83%). For analytical purposes, a small sample of **7** was recrystallized from Et_2O: mp 93−95 °C; ^{1}H NMR ($CDCl_3$) δ 2.64−2.70 (m, 2H), 2.94−3.02 (m, 1H), 3.03−3.13 (m, 1H), 3.25−3.34 (m, 1H), 3.62−3.70 (m, 1H), 3.85 (s, 6H), 3.96−4.03 (m, 1H), 5.11 (s, 2H), 5.45 (br s, 1H), 6.57 (s, 1H), 6.64 (s, 1H), 7.28−7.38 (m, 5H). Anal. Calcd for $C_{20}H_{24}N_2O_4$: C, 67.40; H, 6.79; N, 7.86. Found: C, 67.13; H, 6.58; N, 7.61.

1-Aminomethyl-6,7-dimethoxy-1,2,3,4-tetrahydroisoquinoline dihydrobromide (8·2HBr). Compound **7** (3.56 g, 10 mmol) was suspended in 33% hydrobromic acid in acetic acid (15 mL), and the mixture was heated gently with occasional shaking until all of the substance had been dissolved. The mixture was allowed to stand at ambient temperature for 30 min, and Et_2O (30 mL) was then added. The crystalline dihydrobromide salt of **8** that formed was filtered off, washed with a mixture of MeOH and Et_2O, dried, and recrystallized from MeOH−H_2O−Et_2O: yield 2.99 g (78%); mp 268−269 °C; ^{1}H NMR (D_2O) δ 3.10 (t, 2H, J = 6.6 Hz), 3.52−3.70 (m, 3H), 3.75 (dd, 1H, J = 8.1, 14.6 Hz), 3.87 (s, 6H), 4.91 (dd, 1H, J = 4.5, 8.1 Hz), 6.92 (s, 1H), 6.97 (s, 1H). Anal. Calcd for $C_{12}H_{20}Br_2N_2O_2$: C, 37.52; H, 5.25; N, 7.29. Found: C, 37.27; H, 5.06; N, 7.39.

Pure diamine bases **3** and **8** were obtained from the above dihydrohalide salts by alkaline treatment (20% NaOH), extraction ($CHCl_3$), and evaporation under reduced pressure. The free bases were dried in a vacuum desiccator for 24 h before further transformations.

General Procedure for the Preparation of 3-Aryl-8,9-dimethoxy-1,2,3,5,6,10b-hexahydroimidazo[5,1-*a*]isoquinolines (9, 11, 12a−i) and 3-Aryl-1,2,3,5,10,10a-hexahydroimidazo[1,5-*b*]isoquinolines (10, 13, 14a−i). To a solution of diamine base **3** or **8** (3 mmol) in absolute MeOH (25 mL) was added an equivalent amount of aromatic aldehyde (for liquid aldehydes, a freshly distilled sample was used), and the mixture was allowed to stand at ambient temperature for 1 h. The solvent was evaporated off and the oily product crystallized on treatment with Et_2O or *n*-hexane. The crystalline products **9a**−**i**, **10a**, and **10c**−**i** were filtered off and recrystallized. In the case of **10b**, the evaporation was repeated after the addition of toluene (10 mL), and the oily product was dried in a vacuum desiccator for 24 h. The NMR spectrum proved that the purity of this compound was greater than 95%. All of the recrystallized new compounds **(9a**−**i**, **10a**, and **10c**−**i**) gave satisfactory data on elemental analysis (C, H, N ± 0.3%). The physical data on compounds **9** and **10** are listed in Table S8 in the Supporting Information.

Computational Methodology. The conformational search protocol comprised a stochastic search using MMFF94 implemented in the Chemical Computing Group's MOE software. The ab initio calculations were carried out with Gaussian 94 at the HF/3-21G*//HF/6-31G* level. The NBO analysis was performed by using the NBO 3.1 software implemented in Gaussian 94 with default parameters. The overlapping NBO orbitals were visualized with the molecular graphics package MOLEKEL.[32]

Acknowledgment. We thank the Hungarian Research Foundation (OTKA No. TS 040888) for financial support.

Supporting Information Available: Cartesian coordinates and HF energies for **11**−**14**. Donor−acceptor stabilization energies obtained from the second-order perturbation theory analysis of the Fock matrix in the NBO basis. The off-diagonal Fock matrix elements in the NBO basis. Donor−acceptor orbital energy differences. Polarization coefficients of the C3-associated antibonding orbitals. Physical data on compounds **9**, **11**, **12** and **10**, **13**, and **14**. Selected characteristic ^{1}H chemical shifts (ppm, δ_{TMS} = 0 ppm) for Compounds **9a**−**14a**. Experimental free energies and theoretical stabilization energies for epimerizations I and II. Substituent dependence of the polarization coefficients in the C10b-associated antibonding orbitals in **13**. This material is available free of charge via the Internet at http://pubs.acs.org.

JO034417+

(32) Portmann, S.; Lüthi, H. P. *Chimia* **2000**, *54*, 766−770.